

The Conformation of Amine- and Amide-Terminated Poly(Propylene Imine) Dendrimers as Investigated by Molecular Simulation Methods

Patrick Brocorens,[†] Roberto Lazzaroni,[†] and Jean-Luc Brédas^{*,†,‡}

Service de Chimie des Matériaux Nouveaux, Université de Mons-Hainaut, Place du Parc, 20, B-7000 Mons (Belgium), and School of Chemistry and Biochemistry and Center for Organic Photonics and Electronics, Georgia Institute of Technology, Atlanta, Georgia 30332-0400

Received: April 20, 2005; In Final Form: July 18, 2005

The parameters that influence the conformation of poly(propylene imine) dendrimers were investigated by molecular simulations using molecular mechanics and simulated annealing methods. Dendrimers with two types of peripheral units able to communicate via hydrogen bonding—amine and amide moieties—were considered in order to study the role that secondary interactions among the end groups have in the spatial organization of the dendritic branches. Radial atomic density profiles and radial atomic probability distributions were used to extract global properties, such as the degree of packing of the branches, the distribution of the monomers throughout the molecular volume, and the extent and characteristics of the surface region. Information was also obtained about the nature, location, and extent of formation of the hydrogen bonds, as well as their evolution with dendrimer generation and their assembly into networks. The analyses were supported by a detailed investigation of the first two generations, with an emphasis on the relationship between hydrogen bonding and the compactness and stability of the molecules; this allowed us to account for the generational evolution of hydrogen bonding that is experimentally observed in several poly(propylene imine) dendrimers.

I. Introduction

The peculiar globular architecture of dendrimers, together with the large number of terminal functional groups, are recognized as the source of their unique properties. Many dendrimer-based applications assume a large density of end groups on the surface or the availability of cavities inside the framework. However, theoretical and experimental studies report backfolding of branches in flexible dendrimers.^{1–7} As a result, the end groups may be distributed throughout the molecular volume, filling up the cavities and decreasing the functionality of the molecular surface. The location of the end groups is thus the focus of intense studies, which aim both at determining and controlling the end-group positions. In this context, it is generally believed that preferential interactions among the end groups contribute to maintaining the dendritic termini outward, in a thin surface shell where they can optimally interact with each other and with the molecular environment.

One outstanding example of a soft-dendrimer morphology tuned by end-group modification was built in 1994 by Jansen et al. from an amine-terminated poly(propylene imine) dendrimer of the fifth generation (DAB-dendr-(NH₂)₆₄, with DAB referring to the diaminobutane center, and the subscript 64 referring to the number of end groups).⁸ This molecule has dynamic cavities able to trap guest molecules, the process being reversible due to the flexibility of the framework. Jansen et al. were able to make the encapsulation permanent by grafting amino acid derivatives such as L-phenylalanine protected with a *tert*-butoxycarbonyl (*t*-BOC) group on each of the 64 end groups in the presence of the guest molecules. The behavior of this so-called “dendritic box” was explained by a gathering of

the termini on the dendrimer surface to form a tight outer barrier. Its rigidity has been confirmed by NMR relaxation⁸ and (chir)-optical data,^{9,10} and has been attributed to steric crowding of the bulky amino acid derivatives, as well as to a hydrogen bonding network cementing the end groups and keeping them in the periphery.¹¹ The study of lower generations showed that hydrogen bonding increases generationally, so that 87% of the active hydrogen atoms are involved in hydrogen bonds in the fifth-generation system. This evolution was attributed to a generational increase in the local concentration of end groups, which pushes the termini closer to each other.

The DAB-dendr-(NH-*t*-BOC-L-Phe)_{2ⁿ⁺¹} systems, with *n* running from 1 to 5, were also studied by theoretical methods. Cavallo and Fraternali performed molecular dynamics simulations, which indicated proportions of hydrogen bonds between 39% and 51%.¹² Although these values are significantly lower than the experimental values and do not fully reproduce the generational increase of hydrogen bonding (the lowest value was found for the fifth generation), they provide useful information about the hydrogen bonding pattern. For the first four generations, a large amount (between ~38% and ~46%, depending on the generation) of hydrogen bonds is intraresidue (Figure 1), i.e. within end groups, and ~4–9% is interresidue, i.e., between end groups. In the fifth generation, the proportions change markedly, with intraresidue interactions dropping to 24% and the interresidue interactions increasing to 15%. The hypothesis put forward to explain these changes was that in the fifth generation the steric crowding is larger, which impedes the formation of folded intraresidue structures, to the benefit of interresidue interactions. The simulations also showed that no hydrogen bond involves any tertiary amine of the dendritic scaffold.

In each generation of these dendrimers, many hydrogen bonds are present, mainly as intraresidue interactions in low genera-

* Corresponding author.

[†] Université de Mons-Hainaut.

[‡] Georgia Institute of Technology.

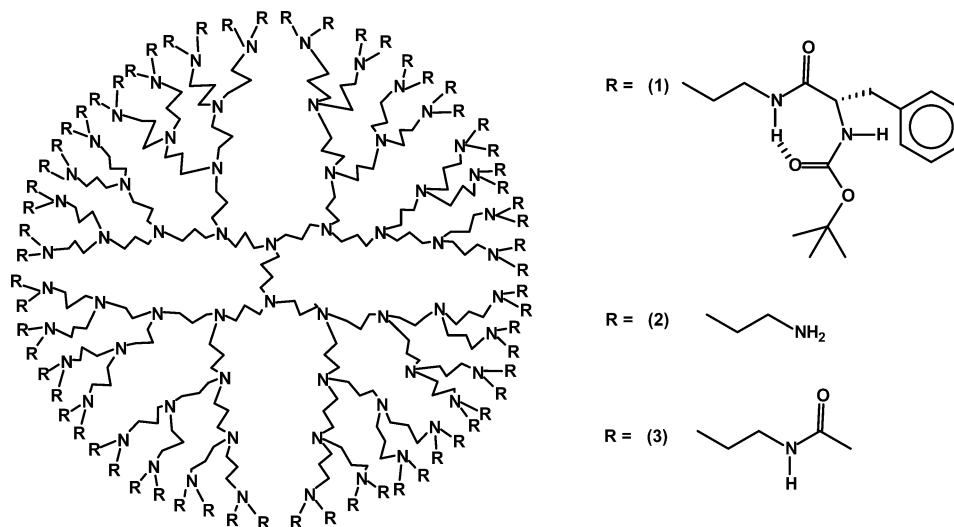


Figure 1. G5 poly(propylene imine) dendrimer capped by L-phenylalanine derivatives (1), here represented with an intrasidue hydrogen bond, amine groups (2), and amide moieties (3).

tions, then with larger proportions of interresidue interactions in higher generations. However, removing the intrasidue interactions by modifying the end groups still allows a high degree of hydrogen bonding to occur, even in the lower generations. A good example is obtained by comparing the following two systems: the DAB-dendr-(NH-*t*-BOC-Gly) $_n$, and DAB-dendr-(NH-3-CO-PROXYL) $_n$ dendrimers, with 3-CO-PROXYL corresponding to 3-carboxy-2,2,5,5-tetramethyl-1-pyrrolidin-1-oxyl;¹¹ the nitroxyl-functionalized dendrimer can establish only interresidue interactions, via the amide functions. In the first generation, the proportion of active hydrogens that is involved in hydrogen bonding is lower in DAB-dendr-(NH-3-CO-PROXYL) $_n$ than in DAB-dendr-(NH-*t*-BOC-Gly) $_4$, i.e., 50% versus 67% (in CH_2Cl_2).¹¹ But, as early as the second generation, the proportions are similar in both molecules, and at the fifth generation, the nitroxyl-functionalized dendrimer has a higher tendency to form hydrogen bonds than the glycine-functionalized dendrimer (hydrogen bond proportions of 90% versus 80%, respectively).

These examples highlight the importance of hydrogen bonding on the dendrimer characteristics. Alongside experimental data, only a few theoretical studies have been devoted to hydrogen bonding in poly(propylene imine) dendrimers, and they are limited to the dendritic box.^{12,13} The goal of our work is to improve the understanding of this issue. For that purpose, two systems in which the end groups are able to interact via hydrogen bonds with different interaction strengths were selected: the amine- and amide-terminated poly(propylene imine) dendrimers, DAB-dendr-(NH $_2$) $_n$ and DAB-dendr-(NHCOCH $_3$) $_n$, i.e., systems 2 and 3 in Figure 1, respectively. Generations 1 to 7 (G1 to G7), i.e., with the number of end groups n doubling at each generation from 4 in G1 to 256 in G7, were modeled by a combination of simulated annealing and molecular mechanics approaches. This allowed us to study the conformational properties of the dendrimers and the extent to which they are influenced by the generation and hydrogen bond strength.

II. Methodology

General Procedure. The molecular simulations were carried out using the Cerius2 molecular modeling system from Accelrys Software Inc.¹⁴ with the Dreiding force field.¹⁵ The dendrimers were built in a stepwise procedure without any geometric

constraint. The procedure started by building a guess structure of the first generation, the geometry of which was relaxed by a molecular mechanics (MM) calculation (see details below). Then, a molecular dynamics (MD) calculation (see details below) was performed in a simulated annealing approach (SA) described as follows: during 0.8 ps, the system was heated from 5 to 800 K by steps of 50 K. Then, a 12.5 ps stay at 800 K allowed the system to undergo conformational changes. The system was cooled for 3.6 ps by steps of 50 K down to 300 K, where a 2 ps simulation allowed for further relaxation, before decreasing again the temperature in 0.8 ps to 5 K by steps of 50 K. Finally, a 0.25 ps stay at 5 K was used to collect a structure for analysis, which was then optimized by MM. This SA procedure was repeated until 15 structures were generated and optimized by MM. One of the most stable structures was then selected, and the end groups were replaced by monomers terminated by end groups to build the next generation. The building-MM-SA-MM procedure was repeated up to the seventh generation.

The method described above allows an extensive exploration of the potential energy surface while driving the search of conformers toward lowest energy regions. The analysis of the fifteen relaxed conformers indicated that the size of the sample is representative enough to extract general trends and qualitative results for the properties of the system. Properties were also extracted from the trajectory generated during the SA.¹⁶ Note that, due to simulation time limitations, the methods used do not guarantee that the exploration of the potential energy surface is complete, nor that the conformers are the most stable ones, or have the highest number of hydrogen bonds. As a result, these methods are expected to underestimate the proportions of hydrogen bonds, and thus their assembling properties; these methods essentially provide qualitative results. To obtain a finer analysis and more quantitative results, a thorough investigation was performed on the first two generations of both dendrimers. It consisted in generating additional conformers with high proportions of hydrogen bonds. Guess geometries, where all the end groups are close enough to each other to be within the range of hydrogen bonding, were built by modifying selected torsions of the branches. The geometries were then relaxed. In the process, the hydrogen bonds that do not allow a proper relaxation of the branches dissociate. Thus, by having initially an overestimated number of hydrogen bonds, it is possible to

obtain the most stable conformers with the highest number of hydrogen bonds by generating only a few different conformers, at least for the lowest generations. For higher generations, this approach is less appropriate, as it becomes burdensome due to the size of the system.

The simulations were performed on isolated molecules in order to focus on the intrinsic factors affecting the morphology. Since no solvent molecules or solvent effect corrections were taken into account, the simulations tend to favor collapsed conformations, i.e., morphologies that could be characteristic of bad solvent conditions. The simulations also correspond to experimental conditions where the solvent is neither a good acceptor nor donor of hydrogen bonds.

To make the analysis of the molecular structures easier, we relied on representations of the dendrimers for which a consistent color coding was applied: the center is in red, and the color of each additional layer of monomers (generation) evolves as follows: purple, blue, turquoise, light green, yellow, light gray, and dark green. The amine capping groups are represented with the nitrogen atoms in pastel blue and the hydrogen atoms in gray; in the amide capping groups, the nitrogen atoms are in pastel blue, the oxygen atoms in pastel red, and the carbon and hydrogen atoms in gray.

Molecular Mechanics Energy Minimizations. The MM energy minimizations were performed with a conjugate gradient algorithm using a convergence criterion of 0.001 kcal/mol.Å. To reduce the computational effort, the number of long-range interactions was decreased: a spline switching function was used to smoothly turn off these interactions between 11 Å and 14 Å. The electrostatic interactions were taken into account by determining the charges on the atoms by means of the charge equilibration algorithm (Qeq),¹⁷ which sets the charge values on the basis of the experimental atomic properties and geometry. As the charge assignment depends on the geometry, the charges have to be recalculated regularly during the geometry optimization process. The charges were equilibrated every 500 minimization steps, until consistency between the charges and the geometry was reached.¹⁸

Molecular Dynamics Simulations. The MD simulations were performed in the NVT ensemble (i.e., particle number, volume, and temperature are kept constant). The Nose–Hoover thermal bath coupling scheme¹⁹ was used with a relaxation time describing the coupling fixed at 0.01 ps. The Verlet velocity algorithm integrated the equations of motion with a 1 fs time step.²⁰ The long-range interaction cutoff was defined by a spline switching method with spline-on and spline-off distances set to 11 Å and 14 Å, respectively. The charges on the atoms were equilibrated every 250 steps by means of Qeq.¹⁷

III. Analysis of the Morphology

In this section, we first investigate how the monomers fill the space. Then, the surface and core regions are defined and described, and their spatial extension evaluated. Next, we study how the monomers assemble with respect to each other. The analyses are based on the radial density profiles of the backbone atoms belonging to the different layers of monomers. Finally, the proportion of end groups located at the surface or trapped in the deepest cavities is investigated with the help of the radial probability distributions of end groups. Except when specified, the discussion and figures refer to the amine-terminated dendrimers, as similar conclusions equally apply to the amide-terminated dendrimers.

1. Packing of the Branches. The radial density profiles of the backbone atoms (C and N) as a function of the distance

from the configurational center (defined from the two central carbon atoms of the diaminobutane center) were determined for G1 to G7 from the SA data. The results are displayed in Figure 2 along with a characteristic conformer for each generation.

The region below 5 Å has a peak followed by a minimum of density. The peak arises from atoms of the molecular center. The minimum corresponds to a zone of exclusion, whose outer boundary is defined by the shortest contacts between nonbonded backbone atoms. Hence, the region that is representative of the packing of the branches, and to which the analysis refers, extends from 5 Å on. The density is largest close to the center, i.e., at about 5 Å, where it exhibits a generational increase until leveling off at the fifth generation. For low-generation dendrimers, this dense central region is directly followed by a smooth decrease of the density when going outward. From the fifth generation on, the densest region broadens radially from the center, thus creating an inner volume of high density that becomes larger with molecular growth. After the density plateau, the density decreases smoothly, as in lower generations.

The degree of branch packing was assessed by means of an ideal model of extended amine-terminated dendrimer, where the volume accessible to the monomers grows for each generation as concentric shells having a thickness equivalent to one monomer length. Assuming that at each growth step the added monomers assemble exclusively in the additional shell, as schematically depicted in Figure 3, the density of backbone atoms in each shell evolves as represented by the black curve in Figure 3. The density shows a minimum in the third shell and increases sharply after the eighth shell. In this “dense shell” model, the densities are 2.4 times (for the seventh layer) to 7.5 times (for the third layer) lower than in the densest regions of our simulated dendrimers. Thus, these dendrimers do not follow the “dense shell” model; they adopt much more compact structures. This behavior is consistent with the “dense core” model, which is promoted by many theoretical studies of flexible dendrimers, where the cavities within the structure are progressively filled up by folded branches when grafting additional layers of monomers. The excluded-volume interactions drive this process, which is characterized by a density that becomes constant when the optimal degree of packing is reached.

Due to the folding of the branches, the volume actually occupied by the molecule is lower than the accessible volume, i.e., the volume defined by the complete extension of the branches. Therefore, the dendrimer has some conformational flexibility to respond to external stimuli. For instance, the inclusion of guests within the dendritic framework would be accompanied by a swelling of the molecule, while upon removal of the guests the structure would deflate. The tuning of the density profile of dendritic electrolytes of the fifth generation, which has been simulated by Welsh and Muthukumar, corresponds to this behavior.²¹ The authors showed that for those topological analogues of poly(propylene imine) dendrimers, a transition occurs from the “dense core” to the “dense shell” model upon a modification of the solvent.

The extended ideal model of Figure 3 indicates that the conformational flexibility would decrease with generation. In the outer shells, the density eventually exceeds the value corresponding to the optimal packing, implying that the monomers are too sterically crowded. The steric interactions have to be relieved, which is only achieved by folding some of the branches. The process decreases the concentration of terminal monomers in the outer shell, while raising their density in the inner shells. The gray curve in Figure 3 represents the generational evolution of the average density of an ideal folded

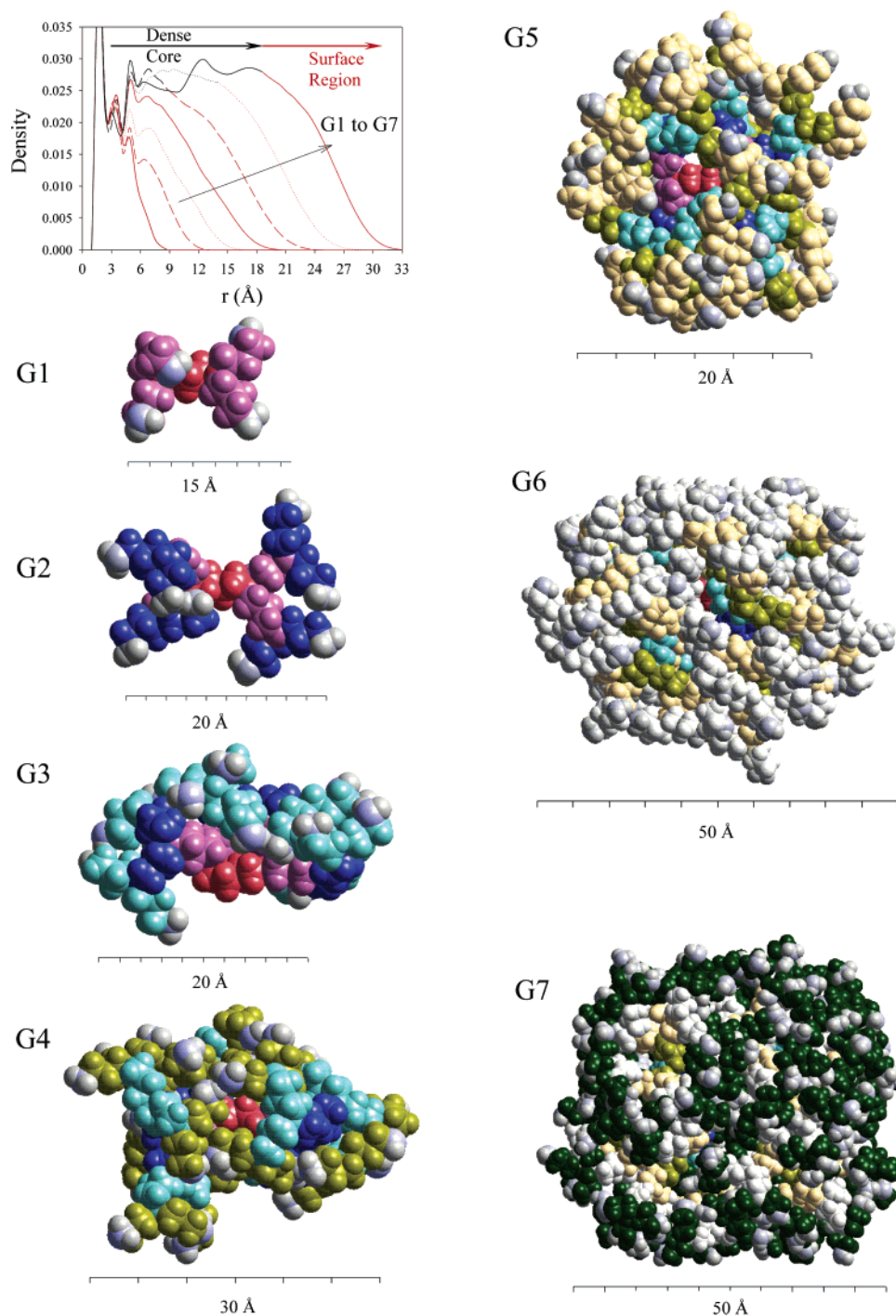


Figure 2. Structure of the amine-terminated dendrimers from G1 to G7, and the corresponding total density profiles with the surface region in red and the dense core in black.

amine-terminated dendrimer for which all monomers are homogeneously dispersed within the whole accessible volume. The average density calculated on the accessible volume still rises with generation and eventually reaches and exceeds the optimal packing density. As the occupied volume gets closer to the accessible volume, the conformational flexibility is expected to decrease, eventually leading to a frozen molecule at the dense-packing limit, beyond which the growth of the dendrimer is prohibited by steric hindrance. According to Figure 3, the limit is at the tenth generation.

However, some features indicate that the dense-packing limit could occur at a lower generation: in G7, the density plateau becomes irregular (Figure 2), with valleys of slightly lower density developing at about 9 Å from the center, and farther

away at about 15 Å. This means that backfolding does not produce a spatial dispersion of the monomers as efficient and homogeneous as assumed in the ideal folded model. This behavior is attributed to multiple folding, which is needed to relieve the central region from an excess of end groups that single foldings tend to induce there, especially in high generations. Indeed, a peripheral monomer getting to the center drags along other peripheral groups due to the very construction of the dendrimer. As the peripheral groups may be in excess for the inner cavities to accommodate them, additional folding is needed to reorient some of them outward. This contributes to decreasing the density of end groups near the center but leads to an opposite trend at intermediate distance, in regions between

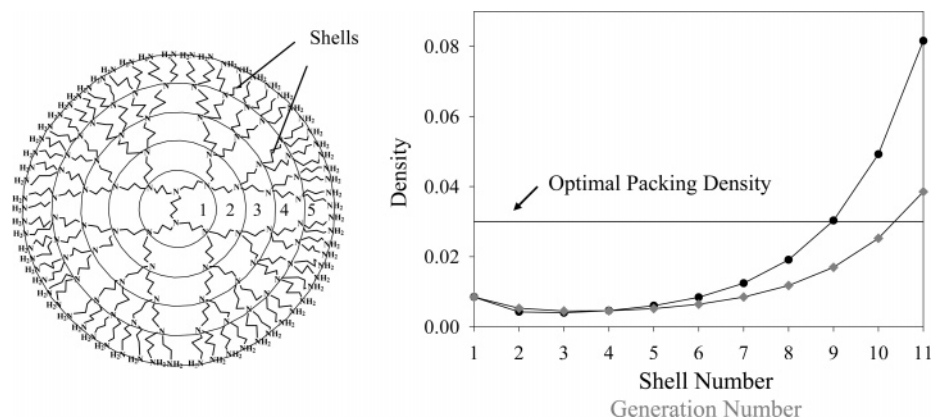


Figure 3. Left: ideal model of an extended amine-terminated dendrimer in which the monomers of each layer are located in concentric shells of thickness equal to one monomer length. Right: evolution of the density of backbone atoms in each shell for such an ideal model (black curve); evolution of the density of backbone atoms as a function of the dendrimer generation when all the monomers are homogeneously dispersed throughout the whole accessible volume of the molecule (gray curve). The density corresponding to an optimal packing of monomers as found in our simulations is indicated by the horizontal line at $0.03 \text{ atoms}/\text{\AA}^3$.

the center and the periphery, which can explain the oscillations observed in the density profile of the highest generations.

2. The Core and Surface Regions. In the characterization of a dendrimer, often the “core” of the molecule is opposed to its “surface”, without always making clear what is meant by “core” and “surface”. It is thus essential to define both regions, which can be done on the basis of the density profiles. The “core” is defined as the region corresponding to the density plateau, where the space occupation is optimized and the atoms are very tightly packed. The molecular “surface” is defined as the region of smooth decrease of the density situated beyond the plateau. This region of imperfect packing of the branches is perforated by channels and hollows, whose interconnections, number, and size increase when going outward. It is intermediate between the sheltered dendrimer core and the surroundings. Based on this definition of the core and surface regions, it is possible to evaluate the thickness of both regions. For the first three generations, only the surface region exists, which extends down to the center (Figure 2); there is no density plateau in those systems. In G4 and G5, a core forms, as the center is progressively sheltered from the external environment, and in higher generations, the extension of the core region increases sharply. For G7, the core extends outward up to 18 \AA , and is followed by the surface region from 18 \AA to 33 \AA . The apparition and growth of the core is accompanied by a generational evolution of the global molecular shape, which is rather open and anisotropic in low generations and progressively evolves toward a globular state in higher generations (Figure 2). This is a phenomenon that has already been reported for soft dendrimers.^{12,22} However, in the next sections, we will show that compact structures also occur in low generations, especially when they are stabilized by strong hydrogen bonds, as in amide-terminated dendrimers.

3. Location of the Monomers. The extent of folding has been examined through the radial density profiles of monomers belonging to different layers, generated in the same way as the total density profiles. The plots are displayed in Figure 4 for the amine-terminated dendrimers (the behavior of the amide-terminated dendrimers is similar); the lines are numbered according to the layer to which the monomers belong, e.g., line 5 in G7 represents the density profile of the monomers of the 5th layer.

In the amine- and amide-terminated dendrimers, backfolding of the branches is confirmed by the density profiles of the terminal monomers. On the whole, those terminal monomers

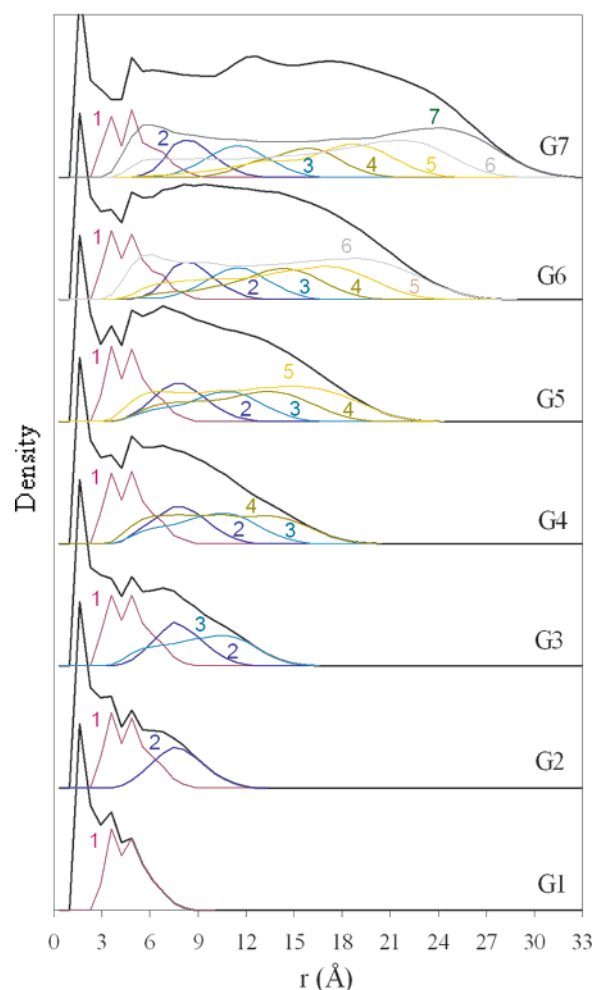


Figure 4. Densities of backbone atoms (C and N) belonging to the different layers of monomers as a function of the distance from the configurational center for seven generations of amine-terminated dendrimers. The total density of backbone atoms is represented as the thick black line.

are dispersed throughout the volume with a rather constant density, from the dense central region to the surface. There, the density shows a smooth decrease, merging with the total density curve in the outermost region, which is populated only by terminal monomers. There are, however, differences between low and high generations. Up to the third generation, while the

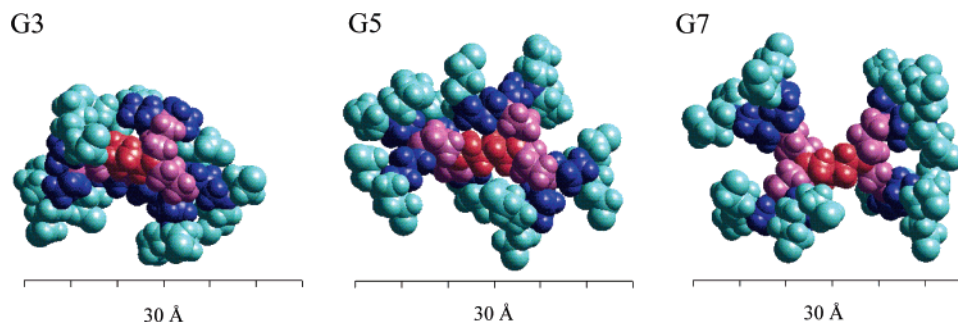


Figure 5. Structure of the molecular center and the monomers of the first three layers for an amine-terminated dendrimer in G3, G5, and G7.

total density increases at each growth step of the dendrimer, the density maximum corresponding to the peripheral units decreases (compare the maxima in line 1 in G1, in line 2 in G2, and in line 3 in G3). One reason for this lies in the elongation of the branches with generation, which favors the formation of loops orienting the end groups back to the center. As the amount of folded branches increases with generation, a more homogeneous dispersion of the monomers throughout the volume is favored. This interpretation is supported by the increase in terminal-group density close to the center when going from G2 to G3 (line 3 in G3 is extending toward the center). Beyond G4, the density of the terminal groups increases throughout the whole volume (compare the height of line 5 in G5, line 6 in G6, and line 7 in G7), and has maxima close to the center and in the outer shell (see, for instance, curve 7 in G7), thus reflecting an intense filling of deep cavities, along with a surface rich in end groups.

When the dendrimer grows, the monomers that were peripheral in earlier generations are buried beneath new layers. They are no longer nearly uniformly dispersed throughout the dendrimer, but are instead characterized by narrower distributions; the deeper the monomers are buried, the narrower the distribution. This is illustrated by comparing the curves corresponding to various layers of monomers in G7. The monomers belonging to the sixth layer also fold back deeply, allowing the end groups to reach the center. These monomers are thus also found throughout the inner layers, but with a density decreasing when approaching the center, as the innermost cavities are mainly occupied by the peripheral groups. The monomers of deeper layers may also fold back to a certain extent, but the amplitude of the folding decreases when going inward. Eventually, backfolding comes to an end; instead, in the innermost layers, the monomers preferentially adopt extended conformations, and their density reaches a maximum at a given distance from the center. As a consequence, there is little overlap between the corresponding density profiles (see line 2 and line 3 in G7, for instance). The extension of the inner monomers is visualized in Figure 5, where the center and the first three layers of an amine-terminated dendrimer are displayed for G3, G5, and G7. The extension of the monomers leads to wider cavities, which are thus able to accommodate a number of end groups that grows with generation.

Together, the extension of the inner layers and the increase of end-group density near the center with increasing generation highlights the role of the central region as a vessel, here filled by the end groups. In this region, the proportion of the global density attributed to the terminal monomers can be fairly high, with values reaching 50% and 55% in the G7 amine- and amide-terminated dendrimers, respectively. When going outward, the proportion of peripheral groups in the total density decreases to a minimum, which is still around 30% and 35% in G7 amine-

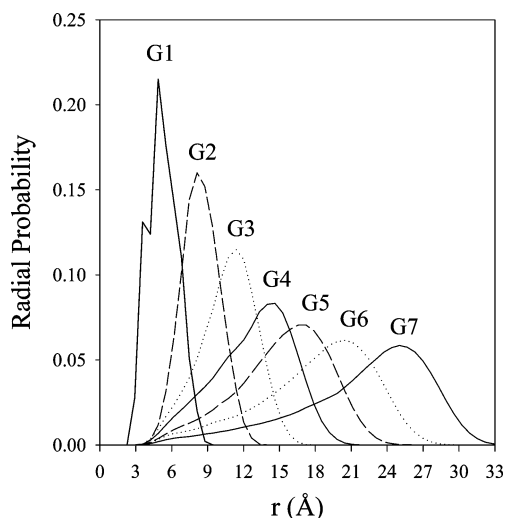


Figure 6. Radial probability distributions of end groups in amine-terminated dendrimers.

and amide-terminated dendrimers, respectively, before increasing again to 100% in the outermost region.

4. Location of the End Groups. The distribution of the dendritic termini as a function of the distance from the center was evaluated by the corresponding radial probability distributions (Figure 6). Note the difference with respect to the radial density profiles seen previously; the probability distributions are a function of the radial density and r^2 . Thus, at constant density of monomers, the farther from the core, the larger the probability to find an end group, since the volume of a shell of given thickness centered on the configurational center increases when going outward.

For all generations, the radial probability of the dendritic termini peaks in the surface region, showing that most end groups are located on the periphery of the molecular volume, despite backfolding. However, the intensity of the peak decreases with generation due to the dispersion of the end groups throughout the whole volume. On the basis of the definition of the surface region given above, all end groups belong to the surface for the first three generations. In the amine-terminated dendrimer, the surface contains 90% of the end groups for G6 and 75% for G7. In the amide-terminated dendrimer, the corresponding values are 75% for G6 and 68% for G7.

The number of end groups that occupy the cavities close to the center was also determined (Table 1). A range of 9 Å from the center has been selected, which roughly corresponds to the region of highest density of end groups near the center. For the amine-terminated dendrimers, 3.8 end groups were found in G3; this number increases generationally to 7.9 in G7. For the amide-terminated dendrimer, the number of end groups evolves from 4.0 in G3 to 7.3 in G7. In low generations, the filling of the

TABLE 1: Number of End Groups within 9 Å from the Center in Amine- and Amide-Terminated Dendrimers

generation	G1	G2	G3	G4	G5	G6	G7
total number of end groups n	4	8	16	32	64	128	256
DAB-dendr-(NH ₂) _n	4	5.3	3.8	4.7	4.9	6.8	7.9
DAB-dendr-(NHCOCH ₃) _n	3.5	3.0	4.0	5.3	5.9	6.4	7.3

cavities is only partial; the cavities belong to the surface region, which extends down to the molecular center. In higher generations, the cavities are filled up in such a way as to optimize space occupation; they belong to the core region. Still, the increase in the number of end groups in the cavities is modest between low and high generations (a 2-fold increase between G3 and G7), compared to the growth of the total number of end groups (a 16-fold increase between G3 and G7), despite the expansion of the volume of the cavities due to the stretching of the inner monomers. Hence, the fraction of end groups sitting in the innermost cavities decreases from ~25% in G3 (4 out of 16) to ~3% in G7 (8 out of 256). The fraction of end groups in the surface region also decreases with generation, thus reflecting the filling of cavities at distances intermediate between the molecular center and the surface.

IV. Hydrogen Bonding

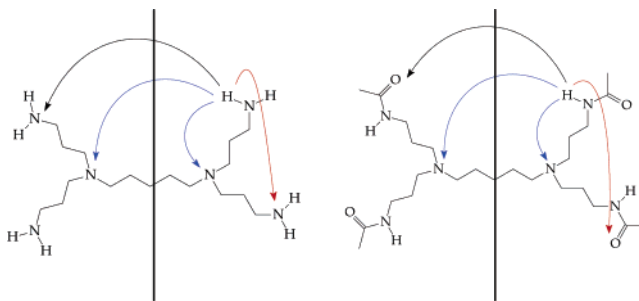
In this section, the hydrogen bond pattern is examined for both dendrimers in order to answer questions that have emerged from the morphology results reported above. As the end groups are dispersed throughout the dendrimer, one may wonder whether the end groups located deep inside the molecule form hydrogen bonds, and if it is the case, with which moiety. Does hydrogen bonding also occur between the end groups and the tertiary amines, or only among the end groups? Do the hydrogen bonds have an organizational effect on the branches?

Important characteristics of the hydrogen bonding pattern were obtained through a detailed analysis of the first two generations. The first generation is ideal to investigate the formation of hydrogen bonds. The system is small, which allows an exhaustive investigation, and contains the smallest structural motif that can form hydrogen bonds and can be traced through all generations. In addition, it has been observed for all generations that most hydrogen bonds involve the two outermost layers of the molecule: the last layer of tertiary amines and the layer of end groups. The first generation contains only these two layers; however, G1 has rather short branches, which limits the way the end groups orient with respect to each other. With G2, this problem does not occur, while the system is still small enough to allow an in-depth study.

For both G1 and G2, only a thorough conformational search was able to generate conformers that have the most stable and dense hydrogen bonding networks. In the following, the discussion focuses, for all generations, on results extracted from the SA simulations, from which only general trends can be extracted. The generational evolution of several characteristics of the hydrogen-bonding pattern is analyzed: first, the proportion of active hydrogens involved in hydrogen bonding is evaluated. Next, the tendency of different acceptor categories to be involved in hydrogen bonding is estimated by means of the active-hydrogens density around the acceptors. Finally, the formation of hydrogen-bond networks is discussed, as well as the possibility for the end groups located deep inside the molecule to form hydrogen bonds.

1. Characteristics of the Hydrogen Bonds: The First Two Generations. The conformers of G1 and G2 for both dendrimers were analyzed on the basis of the type and number of hydrogen bonds and their effect on the stability, compactness, and internal

organization of the molecules.²³ For this purpose, the hydrogen bonds were sorted into three categories, as schematically displayed below for G1: those between branches grafted on the same node (red arrows), those with the tertiary amines (blue arrows), and those between branches grafted on different nodes (black arrows).



In amine-terminated dendrimers, the hydrogen bonds involve the tertiary and primary amines as acceptors. Most of the interactions with tertiary amines occur when a terminal branch folds back and orients its end group toward the tertiary amine to which it is grafted, as in conformers A, B, and C of Figure 7. The interactions between primary amines stabilize the system when involving branches located on two different nodes, as in conformer A of Figure 7. When primary amines grafted on the same node interact, they are accompanied by a hydrogen bond with the node (see the right part of conformer C in Figure 7). Most of the conformers having such interactions are destabilized when compared to similar structures for which hydrogen bonding among neighboring primary amines is absent. The origin of the destabilization can be found in the geometry of the hydrogen bonding pattern. A primary amine is oriented in such a way that one of its two active hydrogens points toward the closest tertiary amine, forming a 6-membered ring, while its second active hydrogen is oriented toward the neighboring primary amine, forming a 10-membered ring. The formation of the 10-membered ring (in C) occurs at the expense of the torsion energy term; for closing such a ring, one of the two branches has to adopt an almost eclipsed configuration, while the branches are staggered in other structures rich in hydrogen bonds, such as A in Figure 7.

As the hydrogen bond formation implies a backfolding of the branches toward the center or toward each other, the radius of gyration tends to decrease with increasing number of hydrogen bonds. A radius of gyration of 4.4 Å and 6.9 Å, determined by SANS measurements in D₂O, has been reported in the literature for G1 and G2, respectively.²⁴ Actually, in our simulations, these values mark the boundary between the conformers with hydrogen bonds and those without. In water, the conformers would thus be moderately extended and with few hydrogen bonds (for example, conformer B in Figure 7 for G1). Since water has some affinity for both the tertiary and primary amines, it competes with the intramolecular interactions as a hydrogen bond donor or acceptor.

Replacing the primary amines by amide groups produces major modifications to the hydrogen bonding pattern. The most stable conformers have hydrogen bonds involving the amide groups only (the most stable conformers of G1 and G2 are displayed in Figure 8). Contrary to what is observed in the amine-terminated dendrimer, the interactions between the end groups are also stabilizing when the interacting branches are grafted on the same node, and not only on different nodes, as illustrated by conformer B in Figure 8. This higher stability can be related to the larger size of the molecular ring formed

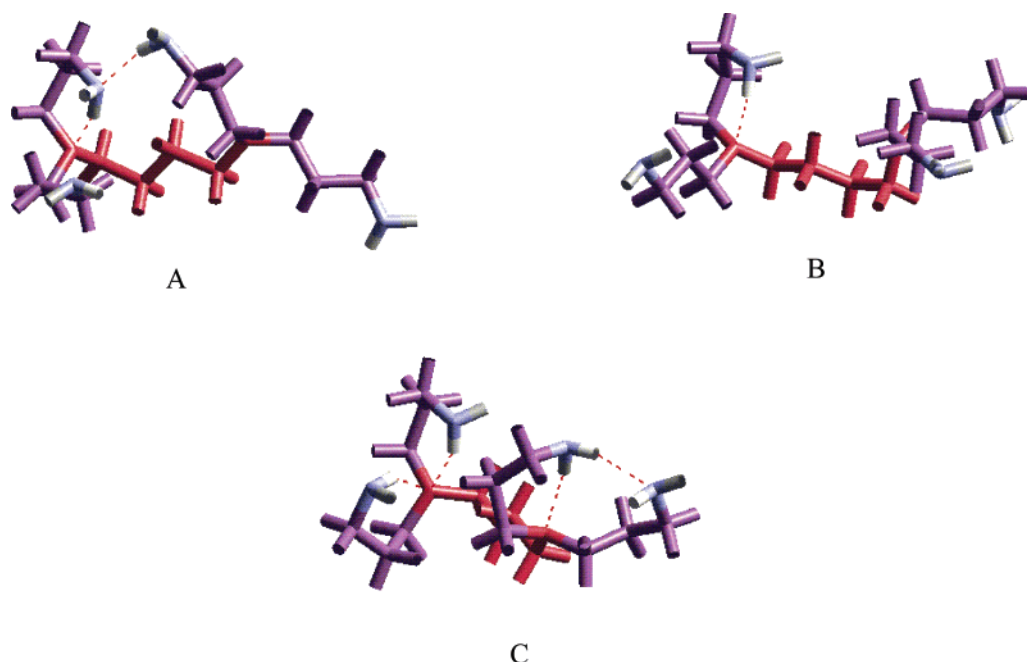


Figure 7. Three representative conformers of the G1 amine-terminated dendrimer, with hydrogen bonds represented by dotted lines.

upon hydrogen bonding, i.e., a 12-membered ring, compared to a 10-membered ring in the amine-terminated dendrimer. The two additional atoms allow a better orientation of the end groups, thus leading to a hydrogen bond as stable as that in dimers of *N*-methylacetamide (NMA).²⁵ Thus, due to the larger flexibility in setting up hydrogen bonds between the amide moieties, the dendrimer branches are able to take different orientations without reducing the stabilizing effect of the network of hydrogen bonds. In conformers rich in hydrogen bonds, the branches can take orientations as extreme as being extended in the prolongation of the center (D for G1, F for G2) or being folded onto the same side of the center (A, B, and C for G1, E for G2).

In G1 and G2, the most stable conformers have a proportion of hydrogen bonds of 50% and 75%, respectively. These values can be compared to experimental data of the nitroxyl-functionalized DAB-dendr-(NH-CO-PROXYL)₄, a dendrimer that establishes hydrogen bonding via its amide moieties.¹¹ The proportion of hydrogen bonding determined in dichloromethane is 50% and ~70% for G1 and G2, respectively. Although the nitroxyl-functionalized dendrimers have an additional layer of substituents in the periphery, the comparison with our systems is relevant since the hydrogen bonding pattern determined in the simulations is expected to be characteristic of many similar systems, as long as the substituents grafted on the amide moieties are not too bulky and do not compete with the amide functionalities for hydrogen bonding (as occurs in the dendritic box¹²). Indeed, the simulations show that the dendrimer termini are directed outward and would easily allow for the growth of the molecular scaffold without major disturbances within the hydrogen bonding pattern. In addition, due to similar proportions of hydrogen bonds in both extended and compact conformers, the molecule has some flexibility to respond to changes brought to the environment or to the outermost layer, while preserving its high proportion of hydrogen bonds. Indeed, in some conformers, a few rotations around the bonds of the backbone are sufficient to evolve from a compact to an extended conformer without breaking any hydrogen bond (for instance, from B to D, in Figure 8). Other conformational changes necessitate a reorganization of the hydrogen bond pattern. This is facilitated by the presence of bifurcated and cooperative

hydrogen bonds, which allow the conformational changes to occur while maintaining the stabilizing effects of a high proportion of hydrogen bonds. For instance, the conversion of B into A can be viewed as the dissociation of the hydrogen bonds between the branches on the same node, followed by the formation of new hydrogen bonds between the branches on opposite nodes. As breaking hydrogen bonds is energetically costly, the reaction path probably involves intermediate conformers such as C, which has both bifurcated and cooperative hydrogen bonds (the stability of C is intermediate between that of conformers without hydrogen bond, and that of A or B, as the high proportion of hydrogen bonds of C (75%) occurs through constraints in the backbone and steric interactions between the branches).

The bifurcations and cooperative interactions between the amide moieties lead to the formation of a network of hydrogen bonds. These effects orient the end groups outward and lead to a segregation between the dendritic layers. Segregation is most marked in structures with high proportion of hydrogen bonds, such as those in Figure 8, where the monomer units belonging to different layers do not mix at all. Some of the conformers are compact (A, B, C, E), and follow the “dense core” model. Others are extended and follow the “dense shell” model; they are less stable than the compact conformers in the “poor solvent conditions” of the simulation. Thus, for low-generation dendrimers, segregation can occur in both models of dendrimer. A smaller proportion of hydrogen bonds leads to more disorder and lack of segregation: the monomers of different layers mix.

Hydrogen bonding can also take place with the tertiary amines. However, no enhancement of the stability is observed, partly due to steric constraints between the acetyl unit and the amine center, as folding brings the capping groups toward the amine center.

2. Generational Evolution of the Hydrogen Bond Pattern.

Hydrogen bonding was first analyzed from the viewpoint of the donors. Table 2 reports the proportion of end groups that is hydrogen bonded, from G1 to G7. The values are averages over the optimized conformers of amine- and amide-terminated dendrimers, respectively, generated via SA. Both systems show a generational increase of the percentage of active hydrogens

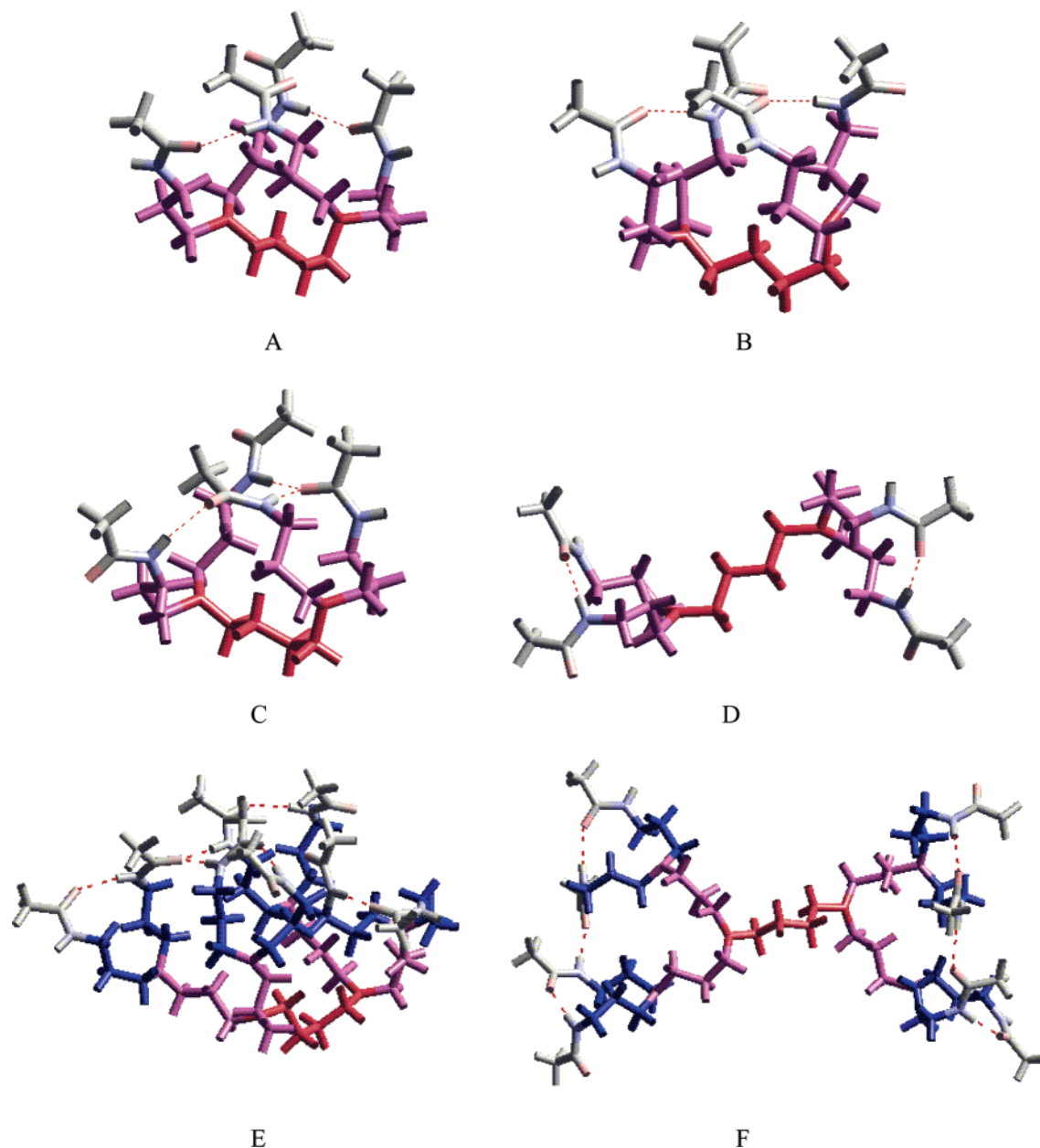


Figure 8. Most stable conformers of the G1 (A, B, C, D) and G2 (E, F) amide-terminated dendrimers with hydrogen bonds represented by dotted lines.

TABLE 2: Proportions of End Groups Involved in Hydrogen Bonds

generation		G1	G2	G3	G4	G5	G6	G7
number of end groups n		4	8	16	32	64	128	256
% end groups in hydrogen bonding	DAB-dendr-(NH ₂) _n :	8.3	8.6	17.9	21.6	27.4	34.4	36.6
	DAB-dendr-(NHCOCH ₃) _n	9.7	17.0	31.8	35.6	35.8	39.5	41.1

involved in hydrogen bonding. For a given generation, the amide-terminated dendrimers have more hydrogen bonds than their amine counterpart, a behavior that can be related to the stronger stability of the hydrogen bonds between the amide moieties.

Hydrogen bonding was also analyzed from the viewpoint of the acceptors. All hydrogen bond acceptors do not participate equally in hydrogen bonding, because either their chemical nature is different—oxygen or nitrogen—or their configurational location makes them more or less accessible to the donors. The acceptors were thus sorted into categories. Each category comprises the acceptors that occupy similar positions on the dendritic scaffold with respect to the configurational center: the nitrogens of the center, those of the first monomer layer, those

of the second monomer layer, etc. For each category, the density of active hydrogens that are around the acceptors within hydrogen bonding range was calculated. A maximum distance of 2.6 Å was used for an acceptor–hydrogen interaction to be considered as a hydrogen bond. The analysis shows that for both dendrimers only the acceptors in the last two layers of monomers (Gth and G-1th) have a sizable concentration of active hydrogens around them. The results corresponding to these categories of acceptors are displayed in Figure 9 from G1 to G7.

The data of Figure 9 reflect the tendency of each category of acceptors to be involved in hydrogen bonding, but not the repartition of the hydrogen bonds between the categories of acceptors—the number of acceptors can vary from one category

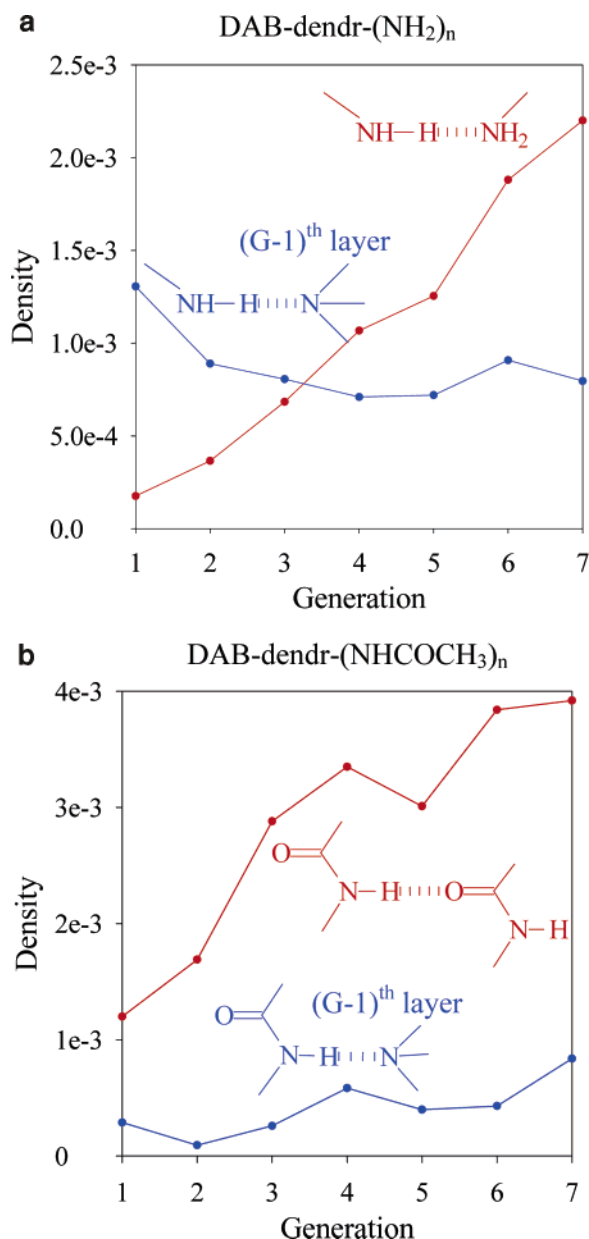


Figure 9. Generational evolution of the density of active hydrogens within hydrogen bonding range around acceptors in the G^{th} and $G-1^{\text{th}}$ layers.

TABLE 3: Proportions of Hydrogen Bonds Occurring with Different Categories of Acceptors

generation	G1	G2	G3	G4	G5	G6	G7
number of end groups n	4	8	16	32	64	128	256
DAB-dendr-(NH ₂) _n							
% H-bond to primary amines	21.2	45.0	62.7	74.1	76.5	79.1	83.0
% H-bond to tertiary amines	78.8	55.0	37.3	25.9	23.5	20.9	17.0
DAB-dendr-(NHCOCH ₃) _n							
% H-bond to amide oxygens	89.0	96.5	94.9	91.2	92.8	80.8	88.4
% H-bond to amide nitrogens	0.4	0.8	0.9	0.8	1.0	14.7	2.1
% H-bond to tertiary amines	10.6	2.7	4.2	8.0	6.2	4.5	9.5

to the other. Table 3 shows the repartition of the hydrogen bonds between categories determined as a function of the chemical nature of the acceptors.

In the amine-terminated dendrimers, most hydrogen bonds take place with the primary amines, or with the tertiary amines of the next to last layer. However, the involvement of those two acceptor categories in hydrogen bonding has a different generational evolution (Figure 9). The proportion of primary amines that accepts a hydrogen bond rises at each generation,

with over a ten-fold increase between G1 and G7. The hydrogen bonds among primary amines are expected to be strongly density-dependent, since, as seen in the detailed study of G1 and G2, they occur preferably between acceptors and donors grafted on different nodes. The generational rise of hydrogen bonding is thus attributed to a generational increase in the density of end groups. While the hydrogen-bonded fraction of primary amines increases with generation, that of tertiary amines is rather constant. As most hydrogen bonds with a tertiary amine involve one of the two end groups that the amine bears, the occurrence of such hydrogen bonds is relatively independent of the density of end groups. As a consequence, the pattern evolves from having mainly the tertiary amines (mainly of the next to last layer) as acceptors in G1 (~80%) to mainly the primary amines in G7 (~80%). The crossing point between the two regimes takes place between G2 and G3 (Table 3).

In amide-terminated dendrimers, most hydrogen bonds are formed with the oxygens of the amide groups (~90%) and the proportion of amide groups involved in hydrogen bonding globally increases with generation. Tertiary amines—those of the next to last layer—are also involved in the hydrogen bond pattern, albeit to a lesser extent (less than 10% of the hydrogen bonds). Their hydrogen bonded fraction also increases with generation.

For both dendrimers, most hydrogen bonds occur in the last two layers; the contribution of the inner tertiary amines is very low because there are fewer inner acceptors than peripheral ones, and also because they are less accessible. The problem of accessibility is especially significant for the amide-terminated dendrimer, as the acetyl units that cap the end groups are bulky enough to maintain the active hydrogens far from the tertiary amines due to steric constraints, or to limit drastically the number of orientations of the amide groups that are favorable to hydrogen bonding.

For both dendrimers, the spatial distribution of hydrogen bonding shows that such bonds occur in the surface region, but also involve end groups trapped within the cavities. Cooperative hydrogen bonds take place among end groups, which self-organize into chains; those chains can be linked by bifurcated hydrogen bonds, leading to the formation of a network of hydrogen bonds that extends inside the molecular volume. From the thorough analysis of G1 and G2 amide-terminated dendrimers, we found different conformers with a network of hydrogen bonds of variable density. Experimentally, however, the proportion of hydrogen bonds measured (on DAB-dendr-(NH-CO-PROXYL)₄)¹¹ corresponds to the maximum found in the simulations (50% in G1, 75% in G2), meaning that the dendrimer adopts conformations that are compatible with a network of hydrogen bonds that is as dense as possible. Experimentally, the proportion of hydrogen bonds rises further in higher generations (about 90% in G5). We attribute this behavior to a decrease of the proportion of active hydrogens isolated on the edge of the peripheral shell, i.e., oriented away from acceptor groups. In higher generations where all the end groups pack optimally in a spherical shell, the proportion of hydrogen bonds would converge to 100%. This is the ideal situation where the layers are segregated. Segregation has been observed in the first two generations, where it is compatible with a highly compact morphology. In higher generations, however, segregation is expected to be more limited as it would be accompanied by empty cavities, i.e., less compact morphologies. Indeed, it was seen on the density profiles that backfolding becomes important from G3 on. With backfolding, the total percentage of hydrogen bonds among amide groups is expected

to be lower than 100%, since isolated clusters of end groups trapped in cavities can only have a fraction of their active hydrogens involved in hydrogen bonding with an amide: one, two, or three end groups can have a maximum proportion of hydrogen bonds of 0%, 50%, and 67%, respectively. However, the backfolded branches have also the ability, though to a small extent, to complete their hydrogen bonding network via interactions with tertiary amines, mainly of the next to last layer.

V. Conclusions

In dendrimers, end groups developing secondary interactions are often viewed as an alternative to rigid building blocks for maintaining the end groups in the periphery of the molecule, where they can more easily interact among themselves. We investigated that phenomenon in amine- and amide-terminated poly(propylene imine) dendrimers, i.e., two systems where the end groups are able to communicate via hydrogen bonding. We used techniques of molecular simulation on isolated molecules in the absence of solvent effects, a situation that can be related to the behavior of molecules in a poor, aprotic solvent. Our results show that both dendrimers adopt compact morphologies with folded branches and filled cavities. They thus correspond to the "dense core" model, similar to flexible dendrimers that do not have any preferential interaction between the end groups.

By comparing our results to experimental data obtained in an aprotic solvent, we conclude that, in absence of competition with the solvent for hydrogen bonding, the amide-terminated dendrimers adopt morphologies with the highest number of hydrogen bonds possible, i.e., allowed by the very construction of the molecule. Thus, the amide-terminated dendrimers adopt morphologies that are compatible with both the highest content in hydrogen bonds possible and the "dense core" model. This implies a proper orientation and gathering of the dendritic termini in small local volumes, both phenomena being favored by the flexibility of the branches. In G1 and G2, the end groups aggregate in a single patch of the molecular surface; as a result, a segregation between the layers of the dendrimer occurs. In higher generations, the end groups occupy the whole surface and some of them also accumulate in the inner cavities. Therefore, hydrogen bonding, though somewhat organizing the branches, is not efficient at driving the dendrimer morphology away from the "dense core" model typical of flexible dendrimers. In particular, in high-generation dendrimers, it does not maintain all the end groups to the periphery and does not impede the folding of the branches. The main reason for this is that the end groups encapsulated in cavities can efficiently establish hydrogen bonds with each other. This allows the end groups to be dispersed into the molecular volume while still being hydrogen-bonded, a behavior that promotes an inward extension of the network of hydrogen bonds.

In the amine-terminated dendrimers, the role of hydrogen bonding on the morphology is even weaker (no segregation between layers is observed, whatever the generation) than in the amide-terminated dendrimers, as the hydrogen bonds are weaker, and the inward extension of the network of hydrogen bonds is further favored by the stable interactions with the hydrogen acceptors at the nodes of the scaffold, mainly those of the next to last layer.

The presence of solvent molecules, which can form hydrogen bonds with the nodes and the end groups, or can possibly fill

the cavities is also a relevant factor. We indeed observed in the amide-terminated dendrimers that it is possible to obtain extended conformations with the same content of hydrogen bonds as in the compact ones, suggesting that the morphology can adapt to the surroundings while conserving its network of hydrogen bonds. Further simulations including solvent molecules could bring additional information on this issue and open the way to the study of the critical influence of external factors on dendrimer morphologies.

Acknowledgment. The work in Mons is partly supported by the Belgian Federal Government (IAP Project V/3) and the Belgian National Fund for Scientific Research FNRS/FRFC. The work at Georgia Tech is partly supported by the National Science Foundation and the Georgia Tech Center for Organic Photonics and Electronics.

Supporting Information Available: Morphology/stability/hydrogen bond relationship for conformers of the G1 amine- and amide-terminated dendrimers. This material is available free of charge via the Internet at <http://pubs.acs.org>.

References and Notes

- (1) Lescanec, R. L.; Muthukumar, M. *Macromolecules* **1990**, *23*, 2280.
- (2) Mansfield, M. L.; Klushin, L. I. *Macromolecules* **1993**, *26*, 4262.
- (3) Boris, D.; Rubinstein, M. *Macromolecules* **1996**, *29*, 7251.
- (4) Mourey, T. H.; Turner, S. R.; Rubinstein, M.; Fréchet, J. M. J.; Hawker, C. J.; Wooley, K. L. *Macromolecules* **1992**, *25*, 2401.
- (5) Wooley, K. L.; Klug, C. A.; Tasaki, K.; Schaefer, J. J. *Am. Chem. Soc.* **1997**, *119*, 53.
- (6) De Backer, S.; Prinzie, Y.; Verheijen, W.; Smet, M.; Desmedt, K.; Dehaen, W.; De Schryver, F. C. *J. Phys. Chem. A* **1998**, *102*, 5451.
- (7) Gorman, C. B.; Hager, M. W.; Parkhurst, B. L.; Smith, J. C. *Macromolecules* **1998**, *31*, 815.
- (8) Jansen, J. F. G. A.; de Brabander-van den Berg, E. M. M.; Meijer, E. W. *Science* **1994**, *266*, 1226.
- (9) Jansen, J. F. G. A.; Peerlings, H. W. I.; de Brabander-van den Berg, E. M. M.; Meijer, E. W. *Angew. Chem., Int. Ed. Engl.* **1995**, *34*, 1206.
- (10) Peerlings, H. W. I.; Meijer, E. W. *Chem. Eur. J.* **1997**, *3*, 1563.
- (11) Bosman, A. W. Ph.D. Thesis: *Dendrimers in action: structure, dynamics and functionalization of poly(propylene imine) dendrimers*, University of Technology: Eindhoven, The Netherlands, 1999.
- (12) Cavallo, L.; Fraternali, F. *Chem. Eur. J.* **1998**, *4*, 927.
- (13) Miklis, P.; Cagin, T.; Goddard, W. A., III *J. Am. Chem. Soc.* **1997**, *119*, 7458.
- (14) Accelrys, formerly Molecular Simulation Inc., 9685 Scranton Road, San Diego, CA, 1997.
- (15) Mayo, S. L.; Olafson, B. D.; Goddard, W. A., III *J. Phys. Chem.* **1990**, *94*, 8897.
- (16) The data extracted from the SA simulations were preferred over those obtained from usual MD methods performed at room temperature, after comparative studies were made.
- (17) Rappé, A. K.; Goddard, W. A., III *J. Phys. Chem.* **1991**, *95*, 3358.
- (18) Typical charges calculated with the Qeq method for an extended conformer of an amine- and amide-terminated dendrimer of the first generation are available as Supporting Information.
- (19) Hoover, W. G. *Phys. Rev. A* **1985**, *31*, 1695.
- (20) Verlet, L. *Phys. Rev.* **1967**, *159*, 98.
- (21) Welch, P.; Muthukumar, M. *Macromolecules* **1998**, *31*, 5892.
- (22) Naylor, A. M.; Goddard, W. A., III; Kiefer, G. E.; Tomalia, D. A. *J. Am. Chem. Soc.* **1989**, *111*, 2339.
- (23) Figures describing the morphology/stability/hydrogen bond relationship for the G1 and G2 conformers of the amine- and amide-terminated dendrimers are available as Supporting Information.
- (24) Scherrenberg, R.; Coussens, B.; van Vliet, P.; Edouard, G.; Brackman, J.; de Brabander, E.; Mortensen, K. *Macromolecules* **1998**, *31*, 456.
- (25) The optimized NMA dimer was used as a standard for rating the stability of amide-amide hydrogen bonds, since the hydrogen bond takes place between amide moieties in the absence of any unfavorable orientation effect.